Technical Paper

ISSN 1997-1400 Int. J. Pavement Res. Technol. 7(5):361-368

Predicting Fatigue Damage of Asphalt Concrete Using a Cohesive Zone Model

Guanglai Jin[1+] and Xiaoming Huang[1]

Abstract: This paper describes a bi-linear cohesive zone model to simulate fatigue behavior of asphalt concrete. To demonstrate the gradual degradation of cohesive properties of asphalt concrete under cyclic loading, a fatigue damage evolution law was integrated into the cohesive zone model. The model was then implemented in commercial finite element software ABAQUS using a user-defined subroutine. A damage extrapolation scheme was adopted to reduce computational cost for high-cycle fatigue applications. Based on the proposed model, a flexural beam fatigue test was finally simulated. The fatigue lives and other features of damage evolution obtained through numerical analysis are in consistence with experimental data, which indicates that the proposed cohesive zone model could be applied to predict fatigue damage of asphalt concrete with good accuracy. During the fatigue loading process, stiffness decreases linearly while damage accumulates non-linearly and grows faster with the increase of fatigue damage. The duration of crack propagation stage is much shorter than the damage initiation stage. The tensile stress at the crack tip increases with the propagation of fatigue crack.

DOI: 10.6135/ijprt.org.tw/2014.7(5).361

***Key words**: Asphalt concrete; Cohesive zone model; Crack propagation; Damage extrapolation; Fatigue damage.*

Introduction

Fatigue failure of asphalt concrete is a significant cause of pavement deterioration. Fatigue cracks can extend through the thickness of pavement and reduce structural capacity. There have been various efforts to investigate the fatigue mechanism of asphalt concrete during the past several decades. Much work has been undertaken based on experimental testing, which is often expensive and time consuming [1-2]. Numerical methods have also been developed to predict fatigue lives, such as the fracture mechanics approach [3-4] and continuum damage mechanics approach [5-6]. However, the numerical methods traditionally used have difficulty in integrating the damage initiation stage and crack propagation stage into a continuous process.

Cohesive zone model (CZM) uses a constitutive equation connecting the crack surface tractions and material separations across the crack, see Barrenblatt, Dugdale, and Rice [7-9]. By using CZM, both the damage initiation stage and crack propagation stage can be considered, and crack tip stress singularities can also be eliminated. Until now, CZM has been employed for a wide variety of problems and materials including metals, ceramics, polymers, composites. Nguyen et al. [10] developed a CZM model demonstrating unloading-loading hysteresis. Siegmund [11] simulated fatigue crack growth using an irreversible CZM. The models mentioned above were both flawed by providing no parameters to characterize speed difference of damage accumulation between materials. Maiti et al. [12] simulated fatigue crack propagation in polymeric materials using a bi-linear CZM, which was ruled by an evolution law relating cohesive stiffness, rate of crack opening displacement and loading cycles. Ura et al. [13] proposed a damage-based CZM to simulate fatigue crack growth. Khoramishad et al. [14] developed a bi-linear CZM integrated with a strain-based fatigue damage model to simulate the fatigue failure of adhesively bonded joints. The computational efficiency of the model was improved by using cyclic increment (ΔN) instead of cycle-by-cycle loading.

The CZM has found its way in fracture analysis of asphalt concrete according to recent research materials. Crack propagation of asphalt concrete in indirect tensile test was simulated using a CZM proposed by Soares et al. [15-16]. A rate-dependent power-law CZM was proposed by Song [17] to simulate fracture of asphalt concrete under both mode I and mixed-mode, considering viscoelastic effects. Kim et al. [18] studied the influence of specimen size on fracture of asphalt concrete using a discrete element-CZM coupled method. Caro et al. [19] developed a coupled micromechanical model to study the moisture-induced damage of asphalt concrete. CZM was employed to simulate the fracture between aggregate-matrix interfaces. Fracture process in mastic and aggregate-mastic interfaces of 2D/3D specimens was also investigated by Yin et al. [20]. However, the application of CZM in fatigue analysis of asphalt concrete is limited according to the author's literature review. Kim et al. [21] simulated the fatigue damage and cracking of asphalt concrete using a nonlinear viscoelastic CZM. Based on the variation of fibril geometry, an effective but a little complicated damage evolution function was proposed.

The objective of this study is to predict the fatigue failure of asphalt concrete using a bi-linear CZM. A fatigue damage evolution law recently developed by Jin and Huang [22] was integrated into CZM to indicate the gradual degradation of cohesive properties of asphalt concrete under cyclic loading. The model was then implemented in the finite element software ABAQUS through user-defined mechanical material behavior (UMAT) subroutine. For high-cycle fatigue applications, a damage extrapolation scheme was

[1] School of Transportation, Southeast University, Nanjing, Jiangsu 210096, China.

+ Corresponding Author: E-mail glking_seu@163.com

Note: Submitted February 28, 2014; Revised August 17, 2014; Accepted August 20, 2014.

adopted to reduce computational cost. The model proposed was then used to simulate laboratory fatigue in this paper.

Cohesive Zone Model under Cyclic Loading

This study used a bi-linear cohesive zone model coupled with a damage evolution law to characterize fatigue features of asphalt concrete under cyclic loading. In the simulation, the constitutive relationship of the material was pre-defined by the bi-linear CZM in the first loading cycle, and the damage evolution law was not activated until the unloading took place. As a result, the material constitutive relationship was characterized by bi-linear CZM in the first cycle and damage evolution law during the following cycles, respectively.

Bi-linear Cohesive Zone Model

The bi-linear CZM under monotonic loading is widely used and proved effective for asphalt concrete by Song [17] and Kim [18]. The traction-separation constitutive equations in bi-linear CZM can be written as:

If $t_e < \sigma_c$ or $\delta_e < \delta_c$,

$$t_n = \frac{\sigma_c}{\delta_c}\delta_n \qquad t_s = \frac{\sigma_c}{\delta_c}\delta_s \tag{1}$$

If $\delta_c < \delta_e < \delta_f$,

$$t_n = \sigma_c \frac{1-\dfrac{\delta_e^{\max}}{\delta_f}}{1-\dfrac{\delta_c}{\delta_f}}\frac{\delta_n}{\delta_e^{\max}} \qquad t_s = \sigma_c \frac{1-\dfrac{\delta_e^{\max}}{\delta_f}}{1-\dfrac{\delta_c}{\delta_f}}\frac{\delta_s}{\delta_e^{\max}} \tag{2}$$

where $t_e = \sqrt{{t_s}^2 + {t_n}^2}$ denotes the effective stress, $\delta_e = \sqrt{\delta_s^2 + \delta_n^2}$ denotes the effective displacement, σ_c is the cohesive strength, δ_c is the cohesive length where cohesive traction is maximal, t_n (t_s) is the normal (tangential) traction, δ_n (δ_s) is the normal(tangential) separation, δ_f denotes the critical displacement where complete separation, i.e. zero traction, occurs. $\delta_e^{\max}$ is the maximum effective displacement during the loading process.

Features of the bi-linear constitutive relation defined above are demonstrated by curve OAB in Fig. 1. Under normal loading, cohesive traction increases with separation before the characteristic cohesive length is reached (shown by OA in Fig. 1), and decreases until it approaches zero (shown by AB). Under pure shear loading, the traction-separation curve is similar to that under pure normal loading. The cohesive fracture energy (G_c) is calculated by equalizing the area under the displacement-traction curve (Fig. 1), and can be expressed as

$$G_c = \frac{1}{2}\sigma_c\delta_f \tag{3}$$

Damage Evolution Law

For cyclic loading, the constitutive relationship must be modified

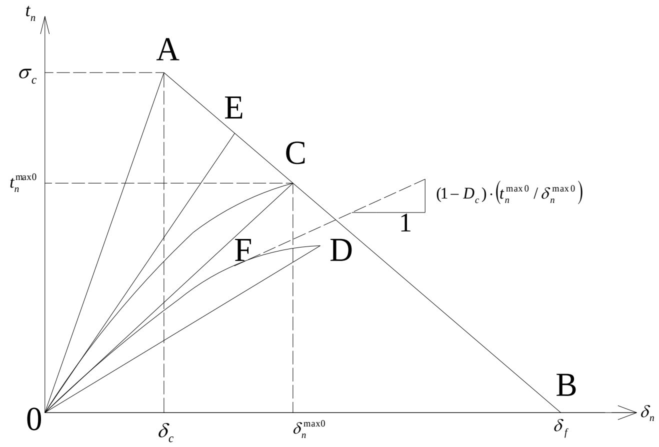

Fig. 1. Traction-separation Relation under Pure Normal Loading [22].

with a damage evolution law that characterizes the progressive degradation of cohesive properties in the cohesive failure zone under subcritical loading. The damage law should incorporate well-known characteristics of continuum damage evolution and these include the following: 1) The increment of damage is related to the increment of deformation as weighted by the current load level. 2) There exists an endurance limit which is a stress level below which cyclic loading can proceed without failure [11].

A fatigue damage variable D_c was used within the proposed constitutive relations to define the degradation of stiffness as follows:

$$\begin{cases} \dfrac{dt_n}{d\delta_n} = (1-D_c)\cdot\left(\dfrac{t_n^{\max 0}}{\delta_n^{\max 0}}\right) \\ \dfrac{dt_s}{d\delta_s} = (1-D_c)\cdot\left(\dfrac{t_s^{\max 0}}{\delta_s^{\max 0}}\right) \end{cases} \tag{4}$$

where D_c is the fatigue damage accumulated in the current loading cycle, $dt_n / d\delta_n$ is the current normal stiffness of the loading stage, $t_n^{\max 0} / \delta_n^{\max 0}$ is the normal stiffness of the unloading stage in the previous cycle.

The feature of this stiffness reduction is shown in Fig. 1. The curve OC represents the previous reloading/unloading cycle and curve OD is the current cycle. Given the fatigue damage D_c at a certain time such as point F in the Fig. 1, the stiffness of the subsequent increment is calculated by $(1-D_c)\cdot\left(t_n^{\max 0} / \delta_n^{\max 0}\right)$. Note that during the unloading stage, no damage is accumulated and both traction and separation return to zero.

To obtain the current state of damage, the derivation of fatigue damage in the current cycle is defined as

$$\begin{cases} \dot{D}_c = a\cdot\left(\dfrac{t_e^{\max}}{\sigma_c} - b\right)^c \cdot \dfrac{t_e}{t_e^{\max 0}}\cdot\dot{\delta}_e & \dot{\delta}_e > 0 \\ D_c = 0 & \dot{\delta}_e < 0 \end{cases} \tag{5}$$

where $\dot{D}_c$ is the accumulation rate of fatigue damage, $\dot{\delta}_e$ is the increment of effective separation, *a*, *b* and *c* are three material parameters, a and c are used for describing the speed of damage accumulation and b for fatigue endurance limit, $t_e^{\max}$ is the maximum effective stress during the whole loading process, $t_e^{\max 0}$ is the maximum effective stress in the previous loading cycle.

Eq. (5) indicates that during the process of any loading cycle, damage is increasing in the loading stage and reset to zero after the unloading begins. The speed of damage accumulation is related to maximum stress level, current stress level, and separation increment. Parameters a, b, and c are employed to describe the different fatigue features of different types of asphalt concrete, among which parameter c is used to characterize the high sensitivity of fatigue life to stress level.

Experimental Test and Finite Element Modeling

Experimental Test

The flexural beam test is often used to investigate the fatigue properties of asphalt concrete. Therefore, fatigue failure of beam specimen was simulated in this study using the CZM presented above. Before the simulation, experimental data was obtained from laboratory fatigue test using flexural beam specimen. The equipment used was MTS810, and the testing condition was stress-controlled mode in three point loading system, under temperature 15°C. The asphalt used was Shell AH-70 with a penetration of 67.8 (0.1 mm) and softening point 49.5°C. The aggregate gradation is listed in Table 1. Semi-sinusoidal loading was applied to the specimen with a frequency of 10Hz. Four stress ratios (0.3, 0.4, 0.5 and 0.6) were used in the test and the experimental data was used to verify the numerical results. Moreover, the indirect tensile test and single-edge notched beam test (SEB) were conducted to determine cohesive strength and fracture energy, respectively. Note that the dimensions of SEB were the same as shown in Fig. 2(a) with an initial crack of 10 mm. The indirect tensile test was conducted according to Chinese Standard Test Methods of Bitumen and Bituminous Mixtures for Highway Engineering (JTG E20-2011). The specimen was a cylinder with a 101.6 mm diameter and a 63.5 mm height, which was fabricated through Marshall Compaction Method. The loading rate of 50 mm/min was used at 15°C and at least three replicates were needed to calculate the cohesive strength.

Finite Element Modeling

The geometry model of the beam specimen is shown in Fig. 2(a). A row of cohesive elements with zero initial thickness was laid along the mid-span section in the finite element model, where fatigue crack would be able to initiate and propagate under cyclic loading. The constitutive response of cohesive element was defined by the damage evolution law through UMAT subroutine as discussed in the Damage Evolution Law section. For bulk material, plane strain elements were laid and the material constitutive relationship was defined as linear elasticity. Fig. 2(b) shows the generated in-plane mesh, in which a higher mesh density was used near the cohesive elements (20 mm in length on both sides) for accuracy consideration.

The mechanical property parameters of asphalt concrete were determined in linear elasticity and CZM. There were eight parameters in total needing to be determined (summarized in Table 2). The elastic modulus E was the flexural modulus obtained by flexural beam test. Cohesive strength σ_c was the tensile strength which was determined by indirect tensile test. Fracture energy G_c was determined by single-edge notched beam test. Failure displacement δ_f was calculated using Eq. (3). Cohesive length δ_c was incorporated to reduce the elastic compliance by adjusting the pre-peak slope of the cohesive law. In other words, as the value of δ_c decreases, the pre-peak slope increases and, as a result, artificial compliance could be reduced. In this paper, $\delta_c = 0.01\delta_f$ was used for asphalt concrete based on previous work by Song [17].

Parameters a and c were used to characterize the fatigue damage evolution behavior of asphalt. Because of the complexity of fatigue behavior, it is usually difficult to determine these parameters directly through test results. Herein an iterative approach was employed, which used an initial guess to generate successive approximations. This approach was also used by Khoramishad et al. [14] to predict fatigue damage in adhesively bonded joints. Note that parameter c indicates the influence of stress level on fatigue lives. Parameter c can be determined first by this iterative approach to match the variance of fatigue lives between any two different stress levels. Then parameter a was determined to obtain accurate fatigue lives.

Parameter b can be calculated by the ratio of fatigue endurance limit (FEL) to the tensile failure strain under which tensile strength is obtained. FEL can be determined through fatigue test under low strain level. In this paper, FEL was assumed based on the research work by Monismith and McLean [23], Thompson and Carpenter [24]. It can be concluded that FEL could vary from 70 to 500 $\mu\varepsilon$ through their work. Assume failure strain equals 4000 $\mu\varepsilon$, the range of parameter b is from 0.018 to 0.125. In order to emphasize the influence of FEL, a relatively large value of 0.15 was used in the simulation.

Damage Extrapolation Scheme for High-cycle Loading

Loading cycles of laboratory fatigue test of asphalt concrete vary from hundreds to thousands. As a result, the cycle-by-cycle iterative calculation can be time-consuming or even computationally prohibitive. In order to reduce the computational cost, a damage extrapolation scheme was employed in the proposed model. Fatigue failure is caused by a large number of loading cycles; thus, the amount of damage accumulated in each cycle is very small. The concept of damage extrapolation is to speed up damage accumulation so that a smaller number of cycles will need to be

Table 1. Aggregate Gradation of Specimen

Sieve Size/mm	16	13.2	9.5	4.75	2.36	1.18	0.6	0.3	0.15	0.075
Passing Percent/%	100	95	70	41.5	28.5	20	14.5	11	8.5	6

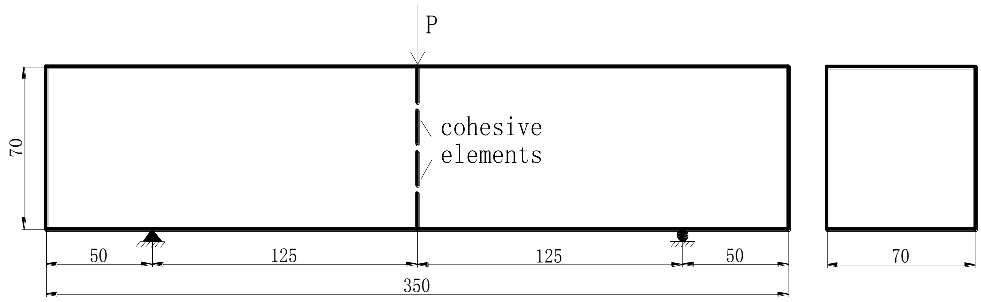

(a)

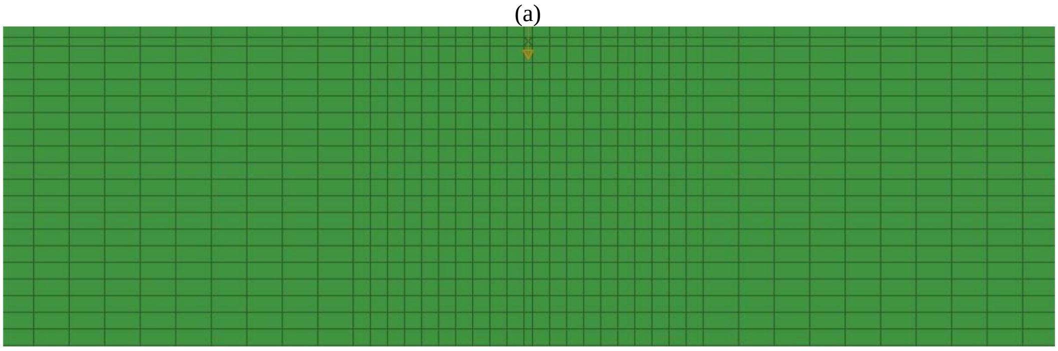

(b)

Fig. 2. (a) Dimensions of the Beam Specimen (Unit of Length: mm); (b) Finite Element Mesh.

Table 2. Mechanical Properties and CZM Parameters of Asphalt Concrete

Cohesive Strength σ_c (MPa)	Cohesive Length δ_c (m)	Failure Displacement δ_f (m)	Flexural Modulus E (MPa)	Poisson Ratio μ	a	b	c
0.798	1.6×10^{-5}	1.6×10^{-3}	496	0.35	4000	0.15	2.6

calculated [13-14]. This paper adopted an effective extrapolation scheme as stated in the following: In order to simulate N cycles of a material with model parameters (a , b , c) where N is relatively large, suppose there exists a damage accumulation scaling function $f(k)$ to convert the model parameters into ($f(k)$ a , b ,c), thus only N/k cycles will need to be calculated explicitly to reach the same amount of fatigue damage. Based on the research of Ural [13], a linear scaling $f(k)=k$ gives good results. The effectiveness of this linear scaling approach was validated in the following paragraph.

Fig. 3 shows the curve of stiffness at the bottom of the mid-span section vs. loading cycles where k = 1, 50, and 100, respectively. The stiffness here is normal stiffness $t_n^{\max0}/\delta_n^{\max0}$, which is calculated at the end of loading stage in cycle n. For k = 1, every parameter in the model was determined following Table 2. For k = 50 and 100, only parameter a needed to be changed into 50×a and 100×a, respectively. After completing the simulation, fatigue lives N and loading cycles n under k = 50, 100 were multiplied by 50, 100 and then shown together with fatigue lives under k = 1. It is observed that the discrepancy between stiffnesses at different extrapolation speeds is small and acceptable with a small k. For k = 50, stiffness decreases to zero almost at the same time as the case of baseline, which indicates that this extrapolation speed has little influence on the time when crack initiation occurs. In the following research in this paper, the value of k is determined as 50.

Discussion

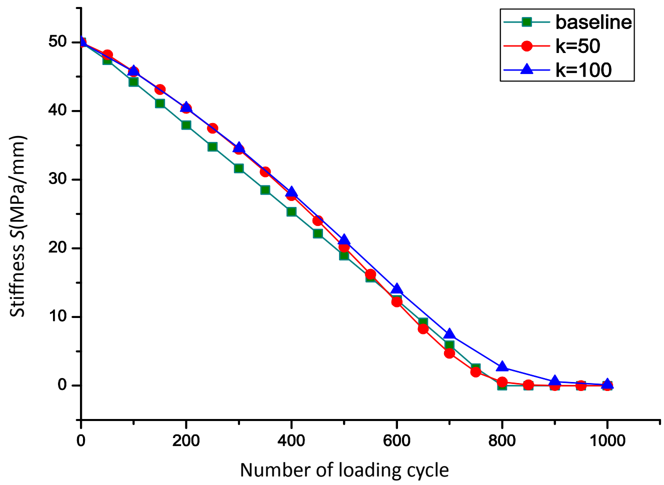

Fig. 3. Stiffness Variations at Different Damage Extrapolation Speeds.

Comparison with Experiments

Fatigue life under a certain stress or strain ratio is one of the main concerns of researchers. Using the presented CZM, fatigue life was predicted and compared with the experimental results (shown as Fig. 4). It can be observed that the predicted fatigue lives are in consistency with measured lives. Moreover, damage extrapolation scheme introduces bigger error for larger fatigue life. However, the maximum error calculated is 11.5% under stress ratio of 0.3, which

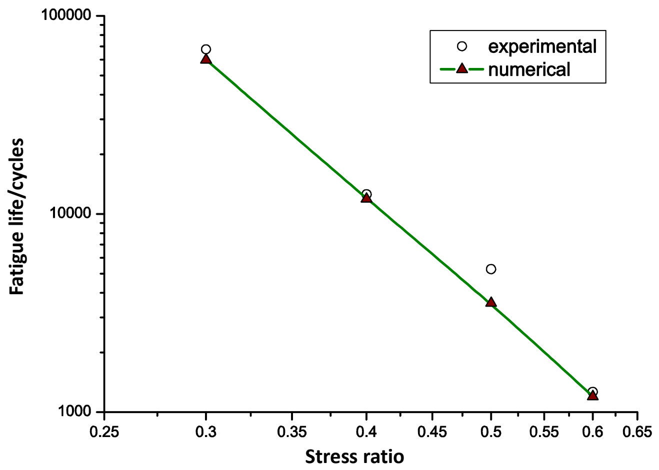

Fig. 4. Comparison of the Predicted and Measured Fatigue Life (log-log Plot).

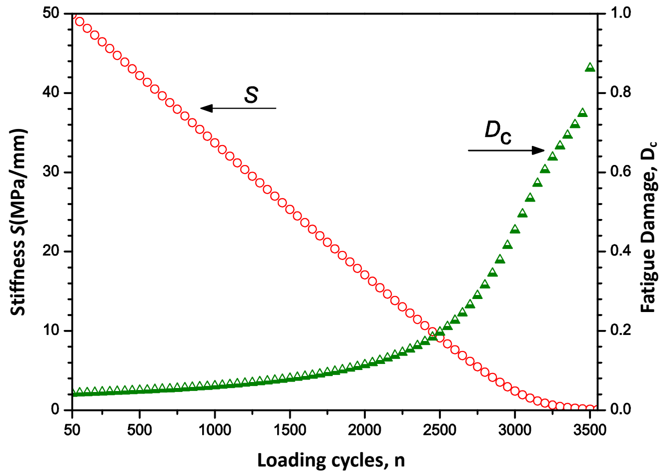

Fig. 5. Variation of Stiffness and Fatigue Damage at the Bottom of the Mid-span Section.

is acceptable for fatigue life prediction. This proves that the proposed model could be safely used to predict the fatigue life of asphalt concrete. It should be noted that the experimental data does not strictly follow a linear distribution in the double logarithmic plot due to the random error under stress ratio of 0.5. However, this error can be mitigated by numerical method.

Characteristics of Fatigue Damage Evolution

Fig. 5 shows the variation of element stiffness and fatigue damage at the bottom of the mid-span section in terms of cycles (stress ratio = 0.5). In the loading process, stiffness decreases at constant speed. Damage accumulates non-linearly and grows faster with the increase of fatigue damage. Laboratory results indicate the two phases of stiffness variation of asphalt concrete under stress-controlled mode: 1) First, stiffness decreases rapidly during the first few cycles. The number of cycles in this phase is relatively small and has little effect on the entire fatigue life, hence this phase will not be taken into consideration. 2) A constant reduction of stiffness takes place in the second phase until destruction of the beam occurs. As a result, it can be concluded that the stiffness variation obtained in the numerical simulation is qualitatively consistent with the experimental result.

The discrepancy between the linear stiffness reduction and the non-linear damage accumulation could be explained by the constitutive relations demonstrated as Eq. (4). Based on the constitutive relationship, the reduction of stiffness in each loading cycle can be given as follows:

$$\Delta S = D_c(n) \cdot S_n = D_c(n+1) \cdot (S_n - \Delta S) \tag{6}$$

where ΔS denotes the reduction of stiffness in each cycle, $D_c(n)$ and $D_c(n+1)$ is the fatigue damage caused in loading step n and $n+1$, respectively. S_n is the material stiffness at the beginning of loading step n. Note that this equation is based on the assumption that reduction of stiffness in each loading cycle is constant.

Eq. (6) can also be written as

$$D_c(n+1) - D_c(n) = D_c(n) \cdot (\frac{\Delta S}{S_n - \Delta S}) \tag{7}$$

In the loading process, $D_c(n)$ keeps increasing and S_n keeps decreasing, hence the right side of the Eq. (7) will keep increasing and the damage increment between two consecutive loading steps will become larger and larger. In other words, the fatigue damage will accumulate faster, leading to a non-linear pattern.

Mechanical Response and Fatigue Crack Growth

Since fatigue damage is related to the constitutive relationship of material to indicate the loss of stiffness, the mechanical response of asphalt concrete changes from cycle to cycle. As shown in Fig. 6 (stress ratio = 0.5), loss of material stiffness leads to significant growth of normal separation and decrease of traction. In fact, stress at the bottom of the mid-span section is decreasing under stress-controlled mode, and the bottom part of the specimen will become softer than other parts due to loss of stiffness, thus it will bear less and less force during the loading process. However, normal traction decreases only from 0.39 to 0.3 in the first 82 percent of fatigue loading cycles, whereas separation increases as much as 6 times. It can be concluded that loss of material stiffness will mainly cause the growth of separation or deformation under stress-controlled mode. In the last 18 percent of fatigue loading cycles, stress decreases rapidly and separation increases significantly until the material loses its load-carrying capacity completely.

The previous analysis of fatigue damage and mechanical response emphasized the bottom of the mid-span section, where the crack initiates and fatigue damage grows fastest. To investigate the damage growth and crack propagation in the whole mid-span section, contour plots are extracted in Fig. 7 to show fatigue damage growth at three loading cycles (N = 3300, 3500, and 3700). The red line represents the locations where fatigue damage reaches 1 and crack propagation occurs. It can be seen that automatic fatigue crack growth in the specimen is well simulated and becomes a natural result of the numerical analysis by use of the proposed CZM. With

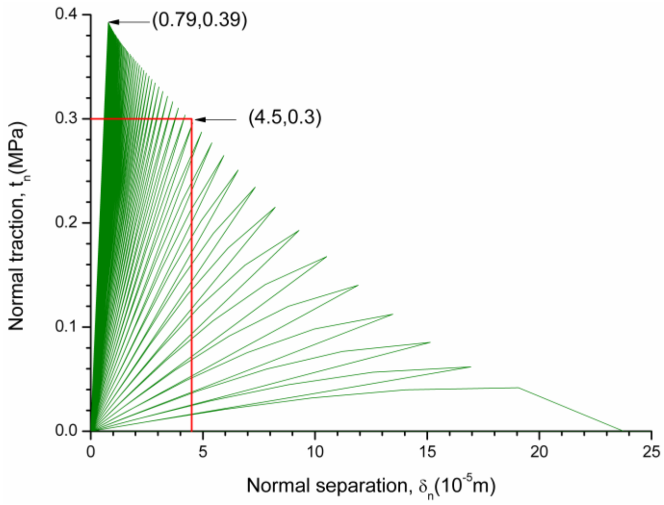

Fig. 6. Mechanical Response of Asphalt Concrete at the Bottom of the Mid-span Section.

this numerical model, the damage initiation stage and crack propagation stage can be investigated as a continuous process without any complicated finite element remeshing.

Because fatigue behavior is simulated cycle by cycle and no crack tip stress singularity exists in the CZM, the present model enables us to capture the transient mechanical response during the fatigue crack propagation stage. Fatigue damage and normal stress along the mid-span section are shown in Figs. 8 and 9, respectively. In the area above the neutral surface of the beam, asphalt concrete is under compression, and fatigue damage will not accumulate. For the area under tension, tensile stress and fatigue damage are becoming larger and larger from the neutral surface to the bottom of the beam. For the area where fatigue damage reaches 1, asphalt concrete has no load-carrying capacity; therefore, tensile stress becomes zero. For N = 3300, damage at the bottom equals 1 and fatigue crack begins. Crack length reaches 5.5 mm in the next 200 cycles (N = 3500) and 19.3 mm in another 200 cycles (N = 3700). Therefore, it can be concluded that the crack length grows rapidly once the initial crack occurs, and the time of crack propagation stage is much shorter than the damage initiation stage. It can also be observed in Fig. 9 that the neutral surface of the beam is moving upwards during the fatigue loading. The locations where tensile stress reaches maximum levels indicate crack tips. Moreover, the tensile stress at the crack tip is increasing when the fatigue crack grows. This is because load-carrying area of the mid-span section is decreasing with the crack propagation, and stress will therefore increase in order to balance the constant fatigue load.

Conclusions

A bi-linear cohesive zone model integrated with a damage evolution law was employed in this paper to investigate the fatigue properties of asphalt concrete. The damage evolution law is related to the stress level and increment of strain. Difference of fatigue characteristics between different types of asphalt concrete were taken into consideration by using three material parameters. A dynamic constitutional relationship was defined based on this damage evolution law. The flexural beam fatigue test was simulated,

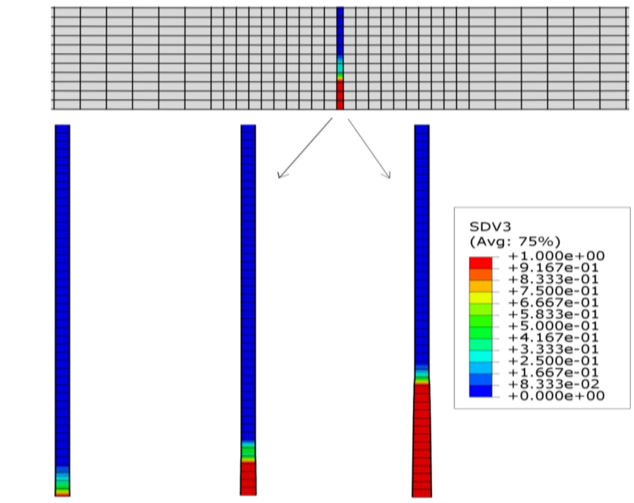

Fig. 7. Contour Plots of Fatigue Damage in the Mid-span Section in Different Loading Cycles (SDV3 Represents Fatigue Damage).

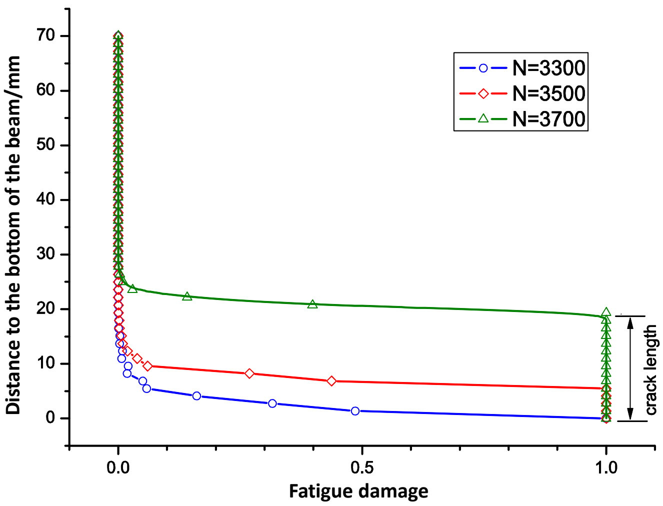

Fig. 8. Distribution of Fatigue Damage in the Mid-span Section in Different Loading Cycles.

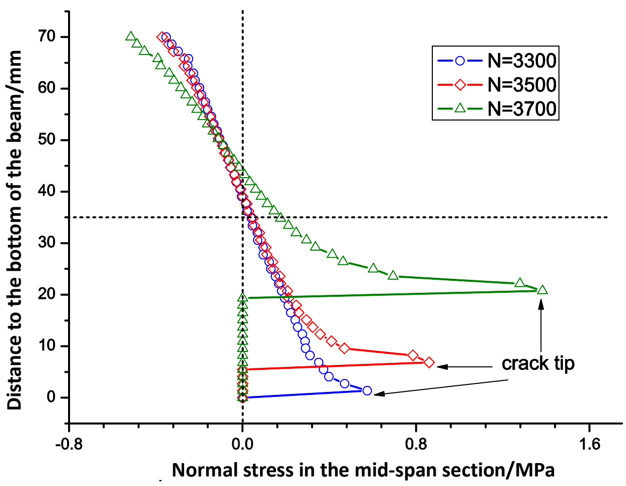

Fig. 9. Distribution of Normal Traction in the Mid-span Section in Different Loading Cycles.

and a damage extrapolation scheme was proposed to improve the computational efficiency. Conclusions of this study could be summarized as following.

Fatigue life obtained by numerical modeling in this study is consistent with experimental data, which indicates the numerical method developed is sufficient in predicting fatigue lives of asphalt concrete.

Characteristics of damage accumulation and mechanical response in the beam were discussed to investigate the mechanism of fatigue failure. The results qualitatively match the experimental data. Stiffness decreases linearly while damage accumulates non-linearly and grows faster with the increase of fatigue damage. Despite the slow decrease of the stress, loss of material stiffness mainly causes growth of material's separation or deformation under stress-controlled mode.

According to the study of fatigue crack growth, damage initiation stage and crack propagation stage can be investigated as a continuous process with the proposed CZM. The duration of crack propagation stage is much shorter than the damage initiation stage in the whole fatigue loading process. The tensile stress at the crack tip increases with the propagation of fatigue crack. However, only plane strain analysis was reported in this paper, and a three-dimensional model should be developed in the future. When it comes to arbitrary crack growth such as mixed-mode cracking, the current model needs to be optimized since the crack propagation path must be predefined in CZM. This problem can also be solved using other approaches such as extended finite element model (XFEM), which will be considered in the future.

Acknowledgement

The authors would like to thank National Natural Science Foundation of China (Grant No. 51178112) for supporting this research project.

References

1. Monismith, C.L., Secor, K.E., and Blackner E.W. (1961). Asphalt Mixture Behavior in Repeated Flexure, *Proceedings of the Association of Asphalt Paving Technologists*, 30, pp. 188-222.
2. Ghuzlan, K.A. and Carpenter, S.H. (2006). Fatigue Damage Analysis in Asphalt Concrete Mixtures Using the Dissipated Energy Approach, *Canadian Journal of Civil Engineering*, 33(7), pp.890-901.
3. Kim, Y.R., Little, D.N., and Lytton, R.L. (2003). Fatigue and Healing Characterization of Asphalt Mixtures, *Journal of Materials in Civil Engineering*, 15(1), pp.75-83.
4. Majidzadeh, K., Kaufmann E.M., and Ramsamooj, D.V. (1971). Application of Fracture Mechanics in the Analysis of Pavement Fatigue, *Proceedings of the Association of Asphalt Paving Technologists*, 40, pp. 227-246.
5. Lee, H.J., Daniel, J.S., and Kim, Y.R. (2000). Continuum Damage Mechanics-based Fracture Model of Asphalt Concrete, *Journal of Materials in Civil Engineering*, 12(2), pp.105-113.
6. Kim, Y.R. (2003). *Mechanistic Fatigue Characterization and Damage Modeling of Asphalt Mixtures*, PhD thesis, Texas A&M University, USA.
7. Barrenblatt, G.I. (1962). The Mathematical Theory of Equilibrium of Cracks in Brittle Fracture, *Advances in Applied Mechanics*, 7(1), pp. 55-129.
8. Dugdale, D.S. (1960). Yielding of Steel Sheets Containing Slits, *Journal of the Mechanics and Physics of Solids*, 8(2), pp. 100–104.
9. Rice, J.R. (1968). Mathematical Analysis in the Mechanics of Fracture, *Fracture: an Advanced Treatise*, 2, pp. 191–311.
10. Nguyen, O., Repetto, E.A., and Ortiz, M. (2001). A Cohesive Model of Fatigue Crack Growth, *Internationl Journal of Fracture*, 110(4), pp. 351-369 ·
11. Siegmund, T. (2004). A Numerical Study of Transient Fatigue Crack Growth by Use of an Irresversible Cohesive Zone Model, *International Journal of Fatigue*, 26(9), pp. 929-939.
12. Maiti, S., Geubelle, P.H. (2005). A Cohesive Model for Fatigue of Polymers, *Engineering Fracture Mechanics*, 69(5), pp. 691-708.
13. Ura, A., Krishnan, V.R. and Papoulia, K.D. (2009). A Cohesive Zone Model for Fatigue Crack Growth for Crack Retardation, *International Journal of Solids and Structures*, 46(11-12), pp. 2453-2262.
14. Khoramishad, H., Crocombe, A.D. and Katnam, K.B. (2010). Predicting Fatigue Damage in Adhesively Bonded Joints using a Cohesive Zone Model, *International Journal of Fatigue*, 32(7), pp.1146-1158.
15. Soares, J.B., Freitas, F.A.C., and Allen, D.H. (2003). Crack Modeling of Asphalt Mixtures Considering Heterogeneity of the Material, *Transportation Research Record*, No. 1832, pp. 113-120.
16. Tvergaard, V. and Hutchinson, J.W. (1992). The Relation between Crack Growth Resistance and Fracture Process Parameters in Elastic-plastic Solids, *Journal of the Mechanics and Physics of Solids*, 40(6), pp.1377-1397.
17. Song, S.H. (2006). Fracture of Asphalt Concrete: A Cohesive Zone Model Approach Considering Viscoelastic Effects, PhD thesis, University of Illinois at Urbana-Champaign, USA.
18. Kim, H., Wagoner, M.P., and Buttlar, W.G. (2009). Numerical Fracture Analysis on the Specimen Size Dependency of Asphalt Concrete Using a Cohesive Softening Model, *Construction and Building Materials*, 23(5), pp. 2112-2120.
19. Caro, S., Masad, E., Bhasin, A., and Little, D. (2010). Micromechanical Modeling of the Influence of Material Properties on Moisture-induced Damage in Asphalt Mixtures, *Construction and Building Materials*, 24(7), pp. 1184-1192.
20. Yin, A.Y., Yang, X.H., and Yang, Z. (2013). 2D and 3D Fracture Modeling of Asphalt Mixture with Randomly Distributed Aggregates and Embedded Cohesive Cracks, *Procedia IUTAM*, 6, pp. 114-122.
21. Kim, Y.R., Allen, D.H., and Little, D.N. (2006). Computational Model to Predict Fatigue Damage Behavior of Asphalt Mixtures under Cyclic Loading, *Transport Research Record*, No. 1970, pp. 196-206.
22. Jin, G.L., Huang, X.M., Zhang, S.L. and Liang, Y.L. (2013). Numerical Study of Fatigue Damage of Asphalt Concrete Using Cohesive Zone Model, *Journal of Southeast University*

(*English Edition*), 29(4), pp. 431-435.

23. Monismith, C.L., McLean, D.B. (1972). Technology of Thick Lift Construction: Structural Design Considerations, *Proceedings of the Association of Asphalt Paving Technologists*, 41, pp. 258-304.

24. Thompson, M.R. and Carpenter, S.H. (2006). Considering Hot-mix-asphalt Fatigue Endurance Limit in Full-depth Mechanistic-empirical Pavement Design. *CD-ROM, Proceedings of the International Conference on Perpetual Pavements*. Columbus, Ohio, USA.